Solvation of CO2 in Water: Effect of RuBP on CO2 Concentration in Bundle Sheath of C-4 Plants

ARTICLE *in* THE JOURNAL OF PHYSICAL CHEMISTRY B · JUNE 2014

Impact Factor: 3.3 · DOI: 10.1021/jp505237s · Source: PubMed

3 AUTHORS:

Tumpa Sadhukhan
Indian Institute of Technology Bombay
5 PUBLICATIONS **6** CITATIONS
SEE PROFILE

Iqbal Latif
Indian Institute of Technology Bombay
12 PUBLICATIONS **83** CITATIONS
SEE PROFILE

Sambhu N Datta
Indian Institute of Technology Bombay
128 PUBLICATIONS **947** CITATIONS
SEE PROFILE

THE JOURNAL OF PHYSICAL CHEMISTRY B

Article

pubs.acs.org/JPCB

Solvation of CO_2 in Water: Effect of RuBP on CO_2 Concentration in Bundle Sheath of C_4 Plants

Tumpa Sadhukhan, Iqbal A. Latif, and Sambhu N. Datta*

Department of Chemistry, Indian Institute of Technology − Bombay, Powai, Mumbai − 400 076, India

Supporting Information

ABSTRACT: An understanding of the temperature-dependence of solubility of carbon dioxide (CO_2) in water is important for many industrial processes. Voluminous work has been done by both quantum chemical methods and molecular dynamics (MD) simulations on the interaction between CO_2 and water, but a quantitative evaluation of solubility remains elusive. In this work, we have approached the problem by considering quantum chemically calculated total energies and thermal energies, and incorporating the effects of mixing, hydrogen bonding, and phonon modes. An overall equation relating the calculated free energy and entropy of mixing with the gas-solution equilibrium constant has been derived. This equation has been iteratively solved to obtain the solubility as functions of temperature and dielectric constant. The calculated solubility versus temperature plot excellently matches the observed plot. Solubility has been shown to increase with dielectric constant, for example, by addition of electrolytes. We have also found that at the experimentally reported concentration of enzyme RuBP in bundle sheath cells of chloroplast in C_4 green plants, the concentration of CO_2 can effectively increase by as much as a factor of 7.1−38.5. This stands in agreement with the observed effective rise in concentration by as much as 10 times.

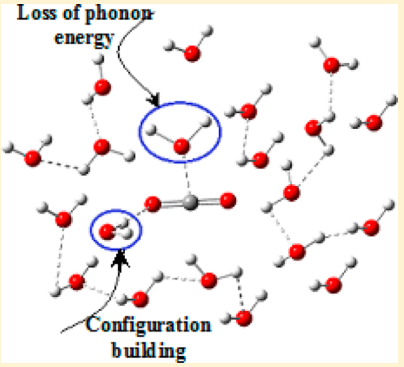

INTRODUCTION

An understanding of the solvation of carbon dioxide in water is important as CO_2 is used in many industrial processes. Solubility has been experimentally determined by a large number of researchers, dating from the 19th century onward. Various advances in this field were reviewed, and the data thereof were compiled by Dodds et al. in 1956.[1] Different empirical functions representing the dependence of solubility upon the polarity of solvent, temperature, and pressure are known, and an idea about these can be easily gleaned from the Internet.

The solvation of CO_2 in water has also been theoretically and computationally investigated, though a quantitative understanding of solubility remains elusive. Past investigations have been fundamentally of two types, namely, quantum chemical calculations and molecular dynamical simulations. Before proceeding further, we present a summary of these advances.

The first quantum chemical advance was made by Jönsson et al.[2] who used ab initio LCAO-MO SCF calculations to show that the hydrogen bond in $CO_2\cdots H_2O$ is stronger when the bonding is of type C···O(water) and the structure is planar, and weaker when the bonding is (carbon dioxide)O···H. These bindings are illustrated in Figure 1. Though the calculations were rather primitive by today's standard, the main conclusion written above still holds good. A detailed study was made much later by Nguyen et al.[3] who used the high-power ab initio MO theory up to the quadratic configuration interaction QCISD-(T)/6-31G(d,p)//MP2/6-31G(d,p) level. These authors also used self-consistent reaction field (SCRF) and polarized continuum model (PCM) model of the continuum electrostatic

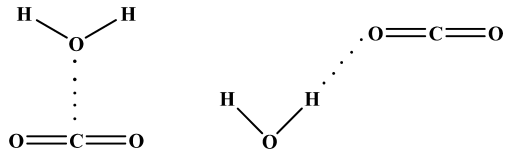

Figure 1. Possible bindings of CO_2 with H_2O.

theory of solvation as well as a mixed treatment coupling the MO results with Monte Carlo and reaction field simulations. They found that four (and three) water molecules are actively involved in the hydration of CO_2 in the gaseous (and aqueous) phase(s). The calculated free energy of the reaction $CO_2 + H_2O \rightarrow H_2CO_3$ in the gaseous phase was 55 kJ mol^{-1}, which predicts an equilibrium constant on the order of 10^{-10}, indicating that, in the absence of basic groups, the solvated carbon dioxide exclusively remains in the neutral though solvated molecular form.

Other studies were made, which have a less direct bearing on solubility. These include the calculation of polarizability from a semiclassical model;[4] study of the surface reactions of CO_2 at the adsorbed water-oxide interface by FTIR spectroscopy and B3LYP/6-31G(d) methodology;[5] comparative calculations of carbon-isotope fractionation in CO_2(g), aqueous carbonates, and carbonate minerals by PBE versus B3LYP, 6-31G(d) versus

Received: May 28, 2014
Revised: June 24, 2014
Published: June 24, 2014

aug-cc-pVDZ, and first solvation shell versus first shell plus a partial second shell methods;[6] and HF/6-31G(d) calculations on stable oxygen isotope fractionation between carbonate ion and water.[7]

On the molecular dynamics (MD) front, a larger number of investigations were done. These involve the use of a variety of force fields. Examples are the simulation of excess volume of aqueous CO_2 at high pressure and temperature;[8] structural properties of aggregates of surfactant, water and carbon dioxide;[9] and thermodynamic properties and interfacial tension of a model water−carbon dioxide system.[10] There have been MD simulations on exotic topics, such as the structural, electronic, and dynamical properties of water in supercritical carbon dioxide;[11] stability of CO_2 hydrates in the presence of unsaturated fluids;[12] molecular diffusion coefficient of dissolved CO_2;[13] carbon dioxide and water at an ionic liquid interface;[14] and liquid−vapor coexistence curve and critical properties of CO_2.[15] There have also been studies in a related area, namely, atmospheric chemistry.[16,17]

Andreoni et al.[18] studied the reaction of CO_2 with water molecules in gas phase by MD simulations combined with density functional theory (DFT) and path metadynamics (MTD). The energies and mechanism of dissociation of H_2CO_3 was studied by Hanna et al.[19] using Car−Parrinello molecular dynamics (CPMD) along with metadynamics. They also studied the role of hydrogen bonding in the dissociation of H_2CO_3 in water clusters by ab initio metadynamics simulation.[20] The stepwise mechanism of the reaction CO_2 and water yielding H_2CO_3 via HCO_3^- was investigated by Stirling and Pápai using ab initio molecular dynamics simulation.[21] Wang and Cao studied the reaction of CO_2 with water including 1−8 water molecules by cluster-continuum model calculations. They found that for 1−4 water molecules, the reaction follows a concerted mechanism whereas for 5−8 water molecules a stepwise mechanism is valid.[22] Stirling also showed by ab initio molecular dynamics simulation that at high pH, the formation of HCO_3^- from CO_2 and OH^- is a reversible reaction. The driving force for the forward reaction is the change in entropy, whereas the backward reaction is fundamentally enthalpic.[23]

A few more direct MD simulations were reported. Patterson et al.[24] investigated the radial distribution function for the oxygen atom of water and the solution free energy for different size parameters and scaling factors. Hydration in the gas phase was studied by Leung et al.[25] using ab initio molecular dynamics simulation. The authors came up with the very important conclusion that carbon dioxide is predominantly hydrophobic, and only a weak coordination to the oxygen atom of water is possible. López-Rendón and Alejandre[26] used a three-point charge model of H_2O with Lennard-Jones repulsion−dispersion interaction and the EMP2 model of CO_2[15] for a MD simulation. They calculated a good value of solubility at 40 °C, 0.23 mol kg^{-1}, under about 1.1 MPa vapor pressure of CO_2. From CPMD simulations, Kirkpatrick et al.[27] reached the conclusion that the presence of CO_2 strengthens the surrounding hydrogen bonding network. These findings fundamentally give support to the finding of Jönsson et al.[2] A quantum mechanical charge field MD study by Rode et al.[28] has been extraordinarily informative. In particular, Rode et al. have estimated the average hydrogen bonding lifetime between CO_2 and H_2O (0.61 ps)[28] to be greater than the hydrogen bonding lifetime of pure water (0.15−0.17 ps).[29] The average number of hydrogen atoms bonded to oxygen of CO_2 has been found to be 0.6. The coordination number can be as large as 4 if the permissible H-bond length is increased to 3.0 Å. The H-bond energy of CO_2−water is −2.28 kcal mol^{-1} compared to −5.94 kcal mol^{-1} for $(H_2O)_2$ at the CCSD/DZP level.

In spite of the voluminous work, a direct conceptual understanding is yet to be developed, and a quantitative explanation is still to be made for the variation of solubility of CO_2 with temperature and dielectric constant. Solubility of CO_2 in water is only a few millimolar per 100 g. of solvent, and therefore the calculation of this quantity is extremely sensitive. The present work aims to fill this gap by taking into account a multitude of physicochemical effects along with quantum chemical calculations at considerable rigor. To avoid confusion, we stress that the present investigation is not on polymerization in the so-called supercritical carbon dioxide or the glass transition of polystyrene in the presence of carbon dioxide,[30,31] but on solution of CO_2 in water under normal thermodynamic conditions.

Our interest in this area arises from the following phenomenon. It is well-known that the C_4 plants generally have a higher rate of CO_2 assimilation than the C_3 plants. The fixation of CO_2 occurs twice in C_4 plants−first in the mesophyll cells and then in the bundle sheath cells. The C_4 plants use phosphoenolpyruvate (PEP) carboxylase instead of RuBP carboxylase for CO_2 fixation in the mesophyll cells and form oxaloacetate. This four-carbon compound (from which the name C_4 plant derives) converts into malates, which pass to bundle sheath cells and form CO_2. The CO_2 liberated in the bundle sheath reacts with enzyme RuBP to produce phosphoglycerate (3-PGA). The phosphogycerate, after a few steps of reactions, converts into glucose-equivalent. The bundle sheath cell is large, and has a smaller surface-to-volume ratio and a dense wall with impermeable layers. These features restrict diffusion of gases. Because of a low concentration of Photosystem II (PSII) in the bundle sheath cell, O_2 production and hence photorespiration are reduced. The enzyme RuBP carboxylase is effectively separated from the atmosphere while remaining in the bundle sheath cell, thus having a higher affinity for CO_2. The bundle sheath cell also gets a supply from surrounding mesophyll cells. These factors lead to a higher CO_2 assimilation. It is known that decarboxylation can yield as much as 10-fold increase in effective CO_2 concentration in bundle sheath cells. A detailed discussion can be found in ref 32, pages 184−192.

The effective CO_2 concentration can increase as a result of the molecule forming a loose complex with the enzyme; this would imply a thermodynamic control. An alternative explanation is that the CO_2 concentration seems to be apparently very high because of kinetic control, that is, a fast supply of malates and a very fast consumption by carboxylase reaction. Our objective here is to show that the effective increase in CO_2 concentration in bundle sheath is at least partially governed by thermodynamic considerations.

Although we have primarily relied on the quantum chemical results, we had to borrow from some of the findings of MD simulations,[24−28] and consider the entropy of mixing, effects of hydrogen bonding at different positions of CO_2, and the contribution from phonon modes. These considerations lead to an expression for the free energy of solvation in terms of the solubility of CO_2 in water as a function of temperature (T). The solution−vapor equilibrium is directly associated with an expression for solvation free energy in terms of solubility. The two expressions can be iteratively solved to find the solubility.

dx.doi.org/10.1021/jp505237s | J. Phys. Chem. B 2014, 118, 8782−8791

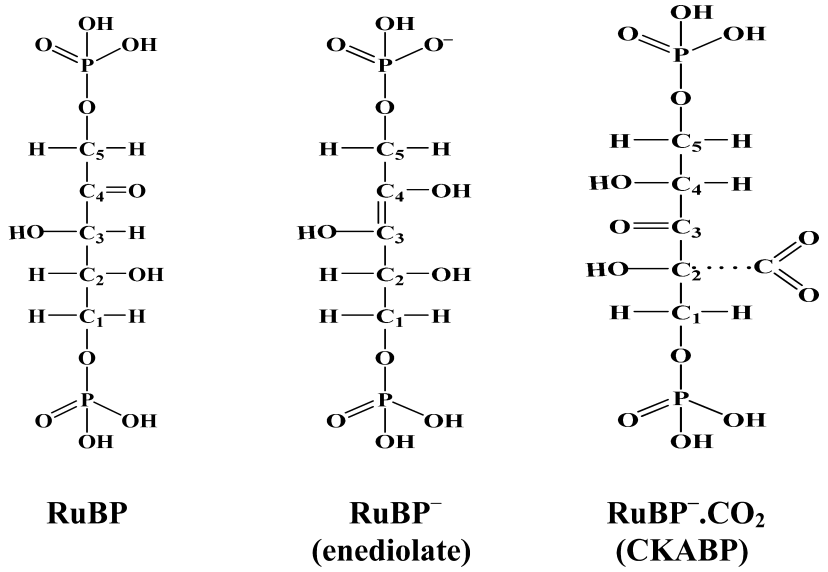

Figure 2. Chemical structures of RuBP, $RuBP^-$, and $RuBP^-{\cdot}CO_2$. For the final step of calculation, explicitly ionized phosphate groups have been considered.

We have also determined the solubility for variation of dielectric constant (ϵ) in a small range.

The effect of RuBP (D-ribulose 1,5-bisphosphate) on CO_2 concentration in bundle sheath cells of C_4 plants has been quantum chemically investigated by considering the equilibrium between (i) RuBP and $RuBP^-$ (the enediolate form) in water, and (ii) $RuBP^-$ (enediolate) and the complex $RuBP^-{\cdot}CO_2$ (2-carboxy-3-keto-D-arabinitol 1,5-bisphosphate or CKABP) at room temperature.[33,34] The chemical structures are shown in Figure 2. For the final step of calculation, explicitly ionized phosphate groups have been considered. We have obtained the fractional concentration of $RuBP^-$ from the first equilibrium constant, and then from the second equilibrium constant, the fractional concentration of $RuBP^-{\cdot}CO_2$ complex. We show that the ratio of total concentration of CO_2 (complex and total solvated inorganic carbon) and the total inorganic CO_2 in solution[35] is in the range of 7.1−38.5 in bundle sheath cells at 298.15 K. An increase of concentration around 10 times is experimentally well founded,[32] and our work provides a simple explanation for this event.

THEORY

For a system in thermodynamic equilibrium, the expectation value of any operator can be evaluated by considering the grand-canonical ensemble of statistical mechanics

$$\langle \mathbf{O} \rangle = \frac{\mathrm{Tr}[e^{-\beta(\mathbf{H}-\mu\mathbf{N})}\mathbf{O}]}{\mathrm{Tr}[e^{-\beta(\mathbf{H}-\mu\mathbf{N})}]} \tag{1}$$

where $\beta = 1/k_B T$, $\mathbf{H}$ is the Hamiltonian, $\mathbf{N}$ is the number operator, μ is the chemical potential, and the notation Tr stands for trace. In this work we are especially interested in the average values of free energy and the population of various configurations. The Hamiltonian is comprised of contributions from electronic, vibrational, rotational, and translational degrees of freedom. For all solvated configurations of CO_2, μ is taken as the same and therefore, without the loss of generality, is equal to zero.

Gaseous Phase. The situation in the gaseous phase becomes exceedingly simple, as the system becomes (generally) dilute with a low level of interaction, and most of the theoretical methodologies and the corresponding computational techniques have been systematically developed. A basic understanding of physical chemistry and the Gaussian 09 (G09) suite of quantum chemical programs[36] suffice a sophisticate treatment. We take a total external pressure of 1 atm, and the saturated vapor pressure of water as p_w atm. The Gibbs free energy per mole of gaseous CO_2 in equilibrium with water vapor is written as

$$G_{CO_2}(g) = G^0_{CO_2}(g) - TS_{mixing}(g) \tag{2}$$

where the free energy of pure CO_2 gas is given by

$$G^0_{CO_2}(g) = E_{tot}(g) + G_{thermal}(g) \tag{3}$$

The latter can be calculated using G09, and it is weakly T-dependent. In particular, $G_{thermal}$ includes translational, rotational, and vibrational energies, the PV contribution, and the corresponding entropy effects. This leaves only the entropy of mixing, which for the gaseous phase can be calculated assuming ideal behavior. We get

$$S_{mixing}(g) = -R\left[\ln(1-p_w) + \frac{p_w}{1-p_w}\ln p_w\right] \tag{4}$$

per mole of carbon dioxide. Standard tables of p_w are available from a variety of sources including the Internet,[37] and the standard free energy of carbon dioxide in the gaseous phase can be easily evaluated.

Aqueous Configurations. While the probability of forming hydrogen bond or a similar C···O bond between CO_2 and H_2O is negligibly small in the gas phase,[25] it can be non-negligible in an aqueous solution at a temperature much below the boiling point of water. This has also been the finding of major MD simulations, and one must necessarily consider a number of configurations (N_c) in which the solvated CO_2 is bound to water albeit weakly, and calculate the free energy of each of these configurations.

The solvated configuration of CO_2 not directly bonded (hydrogen bonded or otherwise C−bonded) to water is

dx.doi.org/10.1021/jp505237s | J. Phys. Chem. B 2014, 118, 8782−8791

ascribed the subscript 1. Other configurations are prepared from a consideration of (carbon dioxide) C···O (water) bonding in "middle," with a relative molecular free energy ε_m per H_2O molecule and a maximum coordination number $n_{m,max}$, and a "terminal" bonding (carbon dioxide) O···H (water) with a relative free energy ε_t per H_2O molecule and a maximum coordination number $n_{t,max}$. Though approximate, the scheme is capable of yielding an accurate average number and the average energy when $\beta|\delta\varepsilon_m| \ll 1$ and similarly, $\beta|\delta\varepsilon_t| \ll 1$ where $\delta\varepsilon$ is the rate of change of free energy with coordination number. The total number of configuration is

$$N_c = 2^{n_{m,max}+n_{t,max}} \tag{5}$$

For $n_{m,max} = 2$ and $n_{t,max} = 4$, one obtains a total of 64 configurations including the nonassociated one (configuration 1).

The water molecules are extensively hydrogen bonded. When solvated CO_2 becomes associated with one water molecule, one must compare the formation of $CO_2{\cdot}H_2O$ bond with the loss of $H_2O{\cdot}H_2O$ bond. This calls for a study of the energies of the reactions

$$CO_2(aq) + (H_2O)_2(aq) \rightarrow CO_2{\cdot}H_2O(m, aq) + H_2O(aq) \tag{6}$$

$$CO_2(aq) + (H_2O)_2(aq) \rightarrow CO_2{\cdot}H_2O(t, aq) + H_2O(aq) \tag{7}$$

The free energy change of the two reactions give $\varepsilon_m^{(0)}$ and $\varepsilon_t^{(0)}$.

A cluster of N' water molecules has 3 translational, 3 rotational and $3N'$ intramolecular vibrational degrees of freedom, and $(6N' - 6)$ phonon modes. When a water molecule is dissociated from the cluster (a representation of the bulk) and becomes associated with the aquated CO_2, not only one hydrogen bond in the bulk is replaced by a new hydrogen bond between CO_2 and the H_2O molecule, but also a maximum of 6 phonon modes are replaced by intramolecular vibrations (and possibly one rotation) when the new hydrogen bonding is strong. For a transient binding as evidenced from molecular dynamics, we consider an average loss of 3 phonon modes. The excess thermal energy, (that is, energy over and above the zero point energy), is in general negligibly small for each intramolecular vibrational mode at around room temperature, as the corresponding frequencies are of the order of 500 cm^{-1} or above, whereas it is about RT for each phonon mode with frequencies on the order of a few tens of wave numbers. Since quantum chemical and molecular dynamical calculations are normally standardized for thermochemistry at 25 °C, the loss of phonon modes requires a correction to be added to the free energy of middle and terminal bindings,

$$\varepsilon_m = \varepsilon_m^{(0)} - 3R(T - 298.15) \tag{8}$$

and

$$\varepsilon_t = \varepsilon_t^{(0)} - 3R(T - 298.15) \tag{9}$$

The nonbonded aqueous configuration $(i = 1)$ has the standard free energy

$$G^0_{CO2}(aq) = E_{CO2}(aq) + G_{thermal}(aq) \tag{10}$$

The quantity $E_{CO2}(aq)$ can be obtained from SCRF (PCM) calculation, whereas $G_{thermal}(aq)$ can be determined by a thermal energy (including vibrational frequency) calculation on the optimized geometry of PCM. Using eq 1 and the number operators $\mathbf{N}_m$ and $\mathbf{N}_t$, one obtains the configurational free energy

$$G_{conf} = (\varepsilon_m < \mathbf{N_m} > + \varepsilon_t < \mathbf{N}_t >)N_{Av} \tag{11}$$

where N_{Av} is the Avogadro number. The ratio of mole fractions of the ith configuration with n_{im} middle and n_{it} terminal hydrogen bonds and the total solvated CO_2 in water is given by

$$\frac{x_i(aq)}{x_{CO_2}(aq)} = \frac{e^{-\beta(n_{im}\varepsilon_m + n_{it}\varepsilon_t)}}{(1 + e^{-\beta\varepsilon_m})^{n_{m,max}}(1 + e^{-\beta\varepsilon_t})^{n_{t,max}}} \tag{12}$$

Here x_i and x_{CO2} are the mole fractions. In our scheme, the degeneracy of states with free energy G_i (the configurational degeneracy) is $g_{im}g_{it}$ where $g_{ip} = \binom{n_{p,max}}{n_{ip}}$, with p standing for m and t. The average coordination number $\langle \mathbf{N}_p \rangle$ is found as

$$\langle \mathbf{N}_p \rangle = \frac{n_{p,max}}{(e^{\beta\varepsilon_p} + 1)} \tag{13}$$

It is important to realize that $G^0_{CO2}(aq)$, ε_m and ε_t are weakly dependent on temperature, and they can be estimated from quantum chemical computations.

Similarly, using eq 1, the free energy of aqueous CO_2 that has been thermally averaged over various bonding configurations is written as

$$\bar{G}^0_{CO2}(aq) = G^0_{CO2}(aq) + G_{conf}(aq) \tag{14}$$

Entropy of Mixing in Aqueous Phase. The free energy of solvated carbon dioxide in the aqueous phase is written as

$$G_{CO2}(aq) = \bar{G}^0_{CO2}(aq) - TS_{mixing}(aq) \tag{15}$$

The entropy of mixing for ideal behavior is

$$\tilde{S}_{mixing}(aq) = -R[x_w \ln x_w + \sum_{i=1}^{N_c} x_i \ln x_i] \tag{16}$$

per mole of solution, where x_w is the mole fraction of water not associated with CO_2 molecules. When $x_w \gg x_i$, $S_{mixing}(aq)$ can be approximated as

$$\tilde{S}_{mixing}(aq) = -R[(1 - x_1)\ln(1 - x_1) + x_1 \ln x_1 + \sum_{i=2}^{N_c} (x_i \ln x_i - x_i)] \tag{17}$$

per mole of solution. The last sum can be neglected when $x_1 \gg x_i$ $(i \neq 1)$. In the present case, however, x_1 and x_i $(i \neq 1)$ are approximately of the same order though $x_1 > x_i$ $(i \neq 1)$. Nevertheless, the species involved lack separate identities, and the quantity $S_{mixing}(aq)$ can be still be estimated from eq 17 without the last sum as discussed below.

Let s be the total solubility of CO_2 in unit ML^{-1}, $f = x_1/x_{CO2}(aq)$ be the fraction of CO_2 not associated with water and N_w be the number of moles of water molecules per liter of pure water. Then $(1 - f)s$ moles of CO_2 molecules are associated with water molecules in 1 L of solution, but the water molecules are only loosely bound and easily become free. As shown by the MD simulations,[28] the average hydrogen bonding lifetime is about half picoseconds and the overall coordination number distribution varies from 10 to 18 with low percent occurrence, so that each water molecule stays bound for a

dx.doi.org/10.1021/jp505237s | J. Phys. Chem. B 2014, 118, 8782−8791

negligible span of time. Thus, the bound water molecules cannot be easily distinguished from the unbound ones. Also, the time average binding is nearly 1:1, with $\bar{n}_i \approx 1.1$ at 300 K.[29] Besides, the solubility s is exceedingly small. Because of these reasons, it turns out to be sensible to consider the associated CO_2 molecules and H_2O molecules together as part of the bulk water and not as separate clusters, and eq 17 without the last sum holds. Thus, the total number of molecules other than the nonassociated CO_2 (that is, the number of associated CO_2 and "free" water) is taken as N_w, the total number of water molecules. This gives the mole fraction $x_1 = fs/(N_w + fs)$ and

$$S_{mixing}(aq) = -\frac{f}{x_1}R[(1 - x_1)\ln(1 - x_1) + x_1 \ln x_1] \quad (18)$$

per mole of solvated CO_2.

Free Energy of Solvation. We now focus on the process of solvation $CO_2(g) \rightarrow CO_2(aq)$ with $\Delta G^{\emptyset} = G_{CO2}(aq) - G_{CO2}(g)$. Thermal equilibration requires

$$\Delta G^{\emptyset} = -RT \ln fsRT/(1 - p_w) \quad (19)$$

Thus, an equality can be established between the difference $G_{CO2}(aq) - G_{CO2}(g)$ from eqs 2 and 15, and the right side of eq 19. We get

$$\Delta G^{\emptyset} = [\bar{G}^0_{CO2}(aq) - G_{CO2}(g)] - TS_{mixing}(aq) \quad (20)$$

As both $\Delta G^{\emptyset}$ in (19) and $S_{mixing}(aq)$ in eq 20 are dependent on s, the equation

$$[\bar{G}^0_{CO2}(aq) - G_{CO2}(g)] + RT\frac{f}{x_1}R[(1 - x_1)\ln(1 - x_1) + x_1 \ln x_1] = -RT \ln fsRT/(1 - p_w) \quad (21)$$

must be iterated for s until self-consistency.

COMPUTATIONAL METHODOLOGY

We have carried out DFT calculations using meta-GGA hybrid functional M06-2X.[38,39] It has 54% Hartree−Fock exchange and an s6 scaling factor of 0.06 for Grimme's long-range dispersion correction.[38,40] The functional B3LYP is normally considered as time-tested for a thermochemical calculation. The performance of B3LYP has been discussed by Mourik and Gdanitz in the context of dispersive effects.[41] It is known that B3LYP is less satisfactory compared to M06-2X for the calculation of energies of systems in which hydrogen bonding and dispersion interactions play a more significant role.[42−44] Although there are a number of other functionals that consider dispersion interactions,[40,43−46] we have selected M06-2X as it has many of the attributes of B3LYP while taking good care of dispersive effects and hydrogen bonding that would be important for the interaction of a primarily nonpolar species like CO_2 with the molecules of solvent.

We have employed 6-311++G(3df,3pd) basis set for all calculations on CO_2, H_2O, and a number of clusters of these species. Calculated total energies have been used to find reaction energies. Solvent effect has been considered by the SCRF-PCM technique. These calculations have been carried out for water as solvent (with dielectric constant 78.39), and also by using other values of dielectric constant. Thermal energy has been estimated from frequency calculations on each species in the gas phase as well as in solution.

We have optimized the molecular geometries of RuBP, $RuBP^-$ (enediolate form) and $RuBP^-{\cdot}CO_2$ in both gaseous and aqueous phases, using 6-311++G(2d,p) basis set (Supporting Information). The SCRF-PCM method has been used for optimization of molecular geometry in the aqueous phase. Finally, the 6-311++G(3df,3pd) basis set has been used to optimize the most stable configurations. As the physiological pH is slightly greater than 7, the anionic forms with fully ionized phosphate groups have been considered for the final calculation. The reason for the choice of the enediolate form is that it is an integral part of the well-established carboxylation scheme,[33,34] which is amply supported by the greater stability of enediolate in water as determined from the quantum chemical calculations.

All quantum chemical calculations have been carried out using the Gaussian 09 (G09) suite of programs.[36]

RESULTS AND DISCUSSION

The calculated free energies of the isolated and aquated species are given in Table S1. Of additional interest is that the C═O bond length calculated at the M06-2X/6-311++G(3df,3pd) level is extremely close to the experimental value,[47] as shown in Table S2, and much better than the bond lengths found from previous many−body calculations. It is not unexpected, as the levels of theory used in the many body methods were rather low, and the basis set employed by us has been significantly large. Our calculations reveal in Table S3 somewhat lower and more realistic hydrogen bond energies both in the gaseous phase and in an aqueous solution. The present calculations give hydrogen bond energy of about 5 kcal mol^{-1} between water molecules. The DFT methodology, however, yields slightly greater vibrational frequencies than experiment[48] as it can be evidenced in Table S4: this is a general trend of DFT calculations with an exchange-correlation functional that has the same form over the entire range of internuclear distance.

Configurational Free Energy. The relative free energy ε of configurations associated with water molecules can be estimated in two ways−quantum chemical calculations[2,3] and molecular dynamical simulations.[24−28] The quantum chemical methods stress the relative stability, the importance of the middle bonding, and the unstable nature of the terminal association. The detailed study by Rode et al.,[28] however, makes it amply transparent that the terminal bonding can have a varying number of coordination numbers in different shells, and as an effect the net bonding becomes non−negligible at 0.6 hydrogen atom per CO_2 with coordination number as large as 4. Because the middle bonding is strong enough, we adopt a puritanical stance and evaluate $\varepsilon_m^{(0)}$from quantum chemical calculations. However, the terminal bonding is weak and long-range, so we take up a holistic approach and estimate $\varepsilon_t^{(0)}$ from the simulated results in ref 28.

Middle and Terminal Bindings. From Table S1, we find for reaction 6, $\varepsilon_m^{(0)} = 0.662(6)$ kcal mol^{-1}. Reaction 7, however, shows a quite large value for $\varepsilon_t^{(0)}$, [$\varepsilon_t^{(0)} = 2.32(9)$ kcal mol^{-1}], which is understandable in view of the findings of Jönsson et al.[2] and Nguyen et al.[3] that a direct hydrogen bonding is not energetically favorable. Therefore, the evaluation of $\varepsilon_t^{(0)}$ is indirect, and it derives from the long-range dispersive interactions with a large number of water molecules in different large hydration shells. With $\langle N_t \rangle = 0.6$ found at $T = 298.15$ K, and $n_{t,max}$ conjectured to be 4 in ref 28, eq 13 yields an effective $\varepsilon_t^{(0)}$ of 1.02(8) kcal mol^{-1}.

dx.doi.org/10.1021/jp505237s | J. Phys. Chem. B 2014, 118, 8782−8791

Table 1. Calculated Free Energies[a]

T (K)	$G_{thermal}$(g) (kcal mol^{-1})	G^0_{CO2}(g) (a.u.)[b]	$G_{thermal}(aq)$ (kcal mol^{-1})	G^0_{CO2}(aq) (a.u.)[c]	ΔG^0 (kcal mol^{-1})
273.15	−4.15	−188.595887	−4.24	−188.593632	1.42
283.15	−4.65	−188.596689	−4.74	−188.594435	1.41
288.15	−4.91	−188.597092	−4.98	−188.594838	1.41
293.15	−5.16	−188.597496	−5.25	−188.595242	1.41
298.15	−5.41	−188.597901	−5.51	−188.595648	1.41
303.15	−5.67	−188.598308	−5.76	−188.596055	1.41
313.15	−6.18	−188.599124	−6.27	−188.596871	1.41

[a]We used 1 a.u. = 627.51 kcal mol^{-1}. [b]G^0_{CO2}(g) = E(DFT) + $G_{thermal}$(g). [c]G^0_{CO2}(aq) = E(PCM) + $G_{thermal}$(aq), eq 10.

Table 2. Calculated Energy Terms[a]

T (K)	p_w (atm)	TS_{mixing}(g) (kcal mol^{-1})[b]	G_{CO2}(g)[c] (a.u.)	G_{conf} (aq) (kcal mol^{-1})	$\bar{G}^0_{CO2}(aq)$ (a.u.)[d]	$\bar{G}^0_{CO2}(aq) - G_{CO2}(g)$ (kcal mol^{-1})
273.15	0.006 03	0.020	−188.595919	0.78	−188.592388	2.22
283.15	0.012 12	0.037	−188.596749	0.85	−188.593076	2.30
288.15	0.016 84	0.050	−188.597171	0.89	−188.593427	2.35
293.15	0.023 09	0.066	−188.597600	0.92	−188.593783	2.40
298.15	0.031 29	0.085	−188.598037	0.94	−188.594145	2.44
303.15	0.041 92	0.109	−188.598482	0.94	−188.594553	2.47
313.15	0.072 89	0.175	−188.599403	1.01	−188.595267	2.60

[a]We used 1 a.u. = 627.51 kcal mol^{-1}. [b]Equation 4. [c]Equation 2. [d]Equation 14.

Phonon Contribution. The MD simulations carried out by Rode et al.[28] are valid for 298.15 K. The phonon-corrected quantities ε_m and ε_t are obtained from eqs 8 and 9. These configurational free energies are to be used to calculate $\bar{n}_m$ and $\bar{n}_t$ from eq 13, and subsequently G_{conf}(aq) from eq 11 for each temperature. Typical calculated values are ε_m = 0.662(6) kcal mol^{-1}, ε_t = 1.027(6) kcal mol^{-1}, (equal to $\varepsilon_m^{(0)}$and $\varepsilon_t^{(0)}$, respectively), $\langle \mathbf{N}_m \rangle$ = 0.49, $\langle \mathbf{N}_t \rangle$ = 0.6, and $G_{conf}(aq)$ = 0.94 kcal mol^{-1} at room temperature.

Factors Determining Solubility. The fraction of "non-associated" CO_2 out of all the CO_2 molecules present in water is given from eq 12 as

$$f = \frac{1}{(1 + e^{-\beta\varepsilon_m})^2 (1 + e^{-\beta\varepsilon_t})^4} \quad (22)$$

with the denominator serving as the relevant partition function.

The solubility of CO_2 in water is determined by a number of factors. These are listed in Tables 1−2. Table 1 shows the free energies of CO_2 in the two phases at different temperatures. The G^0_{CO2}(g) and G^0_{CO2}(aq) values have been obtained by taking E(DFT) and E(PCM) from Table S1. In Table 2 we show the calculations of G_{CO2}(g) and $\bar{G}^0_{CO2}$(aq). Finally, $-TS_{mixing}$(aq) as well as s are iteratively determined from eq 21.

Figure 3 illustrates the influence of these factors. The thermal free energies calculated by Gaussian 09 for the gaseous CO_2 molecule as well as the solvated CO_2 increases almost equally with temperature. This is because they have comparable vibrational frequencies. Thus, one observes from Figure 3 that G^0_{CO2}(aq) − G^0_{CO2}(g) remains almost unchanged with temperature. The term TS_{mixing}(g) increases slowly with temperature in the range 0−40 °C. As the temperature rises, the solubility of CO_2 in water decreases leading to a reduced disorder of mixing. Indeed one finds that with a rise of temperature, $-TS_{mixing}$(aq) increases. One observes a gradual increase in G_{conf} with temperature, as the higher energy configurations (associated with water molecules) become more populated. An overall sharp increase in G_{CO2}(aq) − G_{CO2}(g) is revealed by Figure 3. Entropy in the aqueous phase predominates here; the increase in hydrogen bonding also contributes.

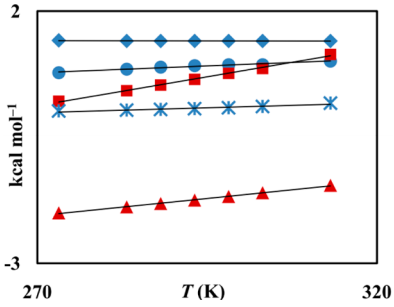

Figure 3. Plots of various thermodynamic parameters (in kcal mol^{-1}) that are considered for CO_2 solubility determination versus T (in K). The different plots are $\Delta G^0 = G^0_{CO2}(aq) - G^0_{CO2}(g)$ ◆; $-TS_{mixing}(aq)$ ▲; G_{conf}(aq) ●; and $G_{CO2}(aq) - G_{CO2}(g)$ ■; $TS_{mixing}(g)$ ∗.

The solubility of CO_2 in water has been iteratively calculated from eq 21. Carbon dioxide in water is always in equilibrium with H_2CO_3, HCO_3^-, and CO_3^{2-}. The equations relating the concentrations of total inorganic carbon ($[CO_2]_{TIC}$) to the concentrations of H_2CO_3, HCO_3^-, and CO_3^{2-} and the calculation of pH are discussed in the Supporting Information. We have taken experimental equilibrium constants from the literature.[49−51] See eqs S1, S2, S3, and S4 in the Supporting Information.

In the present work we have not determined pH. However, we have directly determined $[CO_2]$ in a self-consistent way, from which pH can be estimated from charge balance assuming that the dielectric constant remains more or less unchanged, and then $[HCO_3^-]$ and $[CO_3^{2-}]$can be determined.

The calculated values agree well with the experimental values as shown in Figure 4 and Table 3. As temperature rises, there is a gradual decrease in the solubility. This can be explained from Le Chatelier's principle, as the dissolution of CO_2 in water is an exothermic process. The calculated and experimental s values are comparable at higher temperatures. The difference between these values becomes prominent near 0 °C, which clearly indicates certain additional effects to become operative closely to the freezing point. The most likely explanation is that water

dx.doi.org/10.1021/jp505237s | J. Phys. Chem. B 2014, 118, 8782−8791

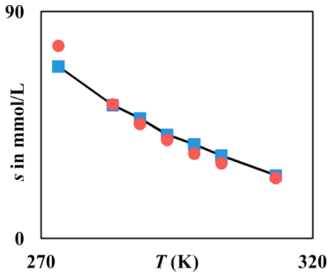

Figure 4. Plot of solubility of CO_2 in water s (mmol/L) versus T (in K): (■) calculated values and (●) experimental values (ref 1).

Table 3. Calculated Solubility of CO_2 in Water at Different Temperature

				s (mmol/L)	
T (K)	$\bar{G}^0_{CO2}(aq) - G_{CO2}(g)$ (kcal mol^{-1})	f	p_w (atm)[a]	calc.	obs.[b]
273.15	2.22	0.43	0.006 03	68.2	76.4
283.15	2.30	0.37	0.012 12	52.9	53.2
288.15	2.35	0.35	0.016 84	47.6	45.4
293.15	2.40	0.32	0.023 09	41.1	39.1
298.15	2.44	0.30	0.031 29	37.3	33.6
303.15	2.47	0.27	0.041 92	32.8	29.8
313.15	2.60	0.23	0.072 89	25.0	23.9

[a]Reference 37. [b]Reference 1.

coexists with ice-like microcrystals. The excess volume becomes large, and some carbon dioxide molecules become trapped in numerous short-range ice structure cavities that are known to exist close to the freezing point.

Influence of Dielectric Constant. We now consider varying the dielectric constant of solvent at 25 °C. The dielectric constant can be increased by adding a small quantity of electrolytes, and we consider only those electrolytes that do not effectively bind with CO_2, such as inorganic salts. The dielectric constant can be decreased by mixing less polar solvents such as alcohols. However, addition of a large quantity of less polar solvent may lead to complications in calculation, as the extent of hydrogen bonding, phonon modes, etc., would be affected.

The saturated vapor pressure of the solvent and the total number of solvent molecules per unit volume remain approximately equal to p_w and N_w when a small quantity of other substances is added. Considering hydrogen bonding only with water, as any possible hydrogen bonding with a less polar solvent is energetically less favorable, the quantities ε_m and ε_t for middle and terminal coordination hardly change for small variation of dielectric constant ε. In consequence, the configurational average G_{conf} and the fraction of nonassociated CO_2 molecules f remain more or less unchanged.

The solubility of CO_2 has been determined in an aqueous solution with various dielectric constants at 298.15 K. The s values calculated iteratively from eq 21 are given in Table 4. The results are obviously less reliable for the lower dielectric constants, and therefore, only reflect the qualitative trend. We find a gradual increase in the solubility of CO_2 with dielectric constant of the medium (Figure 5). This is understandable as an increase in dielectric constant leads to a larger dipole-dielectric interaction that decreases the free energy and leads to a higher solubility. To conclude, it is the internal energy that dictates the variation of solubility with dielectric constant.

Table 4. Calculated Solubility of CO_2 in Different Medium of Different Dielectric Constant at 298.15 K[a]

ε	E(SCRF-PCM)	$G_{thermal}$(sol)	G^0_{CO2}(sol)	s (mmol/L)
100	−188.586885	−0.008775	−188.595660	37.7
78.39	−188.586873	−0.008774	−188.595647	37.3
60	−188.586856	−0.008773	−188.595629	36.7
40	−188.586820	−0.008771	−188.595591	35.6

[a]All energies are in atomic units.

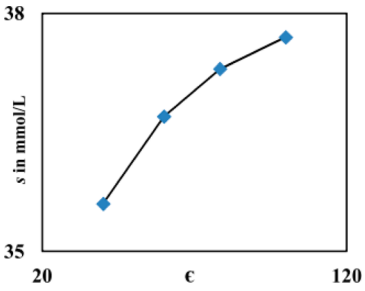

Figure 5. Plot of calculated solubility of CO_2 in water s (mmol/L) versus dielectric constant of solvents ε. The plot is qualitatively correct when ε < 78.39.

Effect of RuBP. We have carried out quantum chemical DFT calculations using M06-2X functional and 6-311++G(3df,3pd) basis set. The "neutral" chemical structures of RuBP, $RuBP^-$, and $RuBP^-{\cdot}CO_2$ are shown in Figure 2. Two stable structures, linear (bent) and puckered, are obtained for each species. For RuBP, $RuBP^-$ (enediolate), and $RuBP^-{\cdot}CO_2$ the puckered form is more stable in the gaseous phase, whereas in the aqueous phase, the puckered form is more stable for RuBP and $RuBP^-{\cdot}CO_2$, but the linear (bent) structure is more stable for $RuBP^-$ (enediolate). The solvated molecular geometries with fully ionized phosphate groups are displayed in Figure 6. Calculated energies are given in Table S5. The reason for the greater stability of the bent configuration for enediolate is that the atom H16 is in interaction with both O7 and O11 (numbering in Figure 6). In the puckered configuration, O11 is away. The carbon atom of CO_2 is loosely attached to C2 of $RuBP^-{\cdot}CO_2$ (see Figure 2). The C2−C(O2) distance is 1.635 Å in the isolated species and 1.577 Å in the solvated structure.

The free energies for the following two reactions are calculated from SCRF-PCM total energies and the thermal free energies:

$$RuBP(aq) + OH^-(aq) \overset{K_1}{=} RuBP^-(aq) + H_2O(aq) \quad (23)$$

$$RuBP^-(aq) + CO_2(aq) \overset{K_2}{=} RuBP^-{\cdot}CO_2(aq) \quad (24)$$

We find for reaction 23, ΔG_1^ϕ = −7.30 kcal mol^{-1}, which yields the equilibrium constant K_1 = 2.25 × 10^5 at 298.15 K, whereas for reaction 24, ΔG_2^ϕ= −13.16 kcal mol^{-1}, which corresponds to K_2 = 4.45 × 10^9. It is interesting to note that El-Hendawy et al.[52] have carried out multiple MD simulations on the diffusion of CO_2 molecules from the enzyme Rubisco bounded to Mg^{2+} cation at 298 K and estimated the activation barrier for carboxylation of $RuBP^-(g)$. From the B3LYP/6-31+G(d,p) level, these authors estimated that the product of carboxylation in vacuo is stable by about 6.8 kcal mol^{-1}. The calculated ΔG_2^ϕ is of this order, though it corresponds to an

dx.doi.org/10.1021/jp505237s | J. Phys. Chem. B 2014, 118, 8782−8791

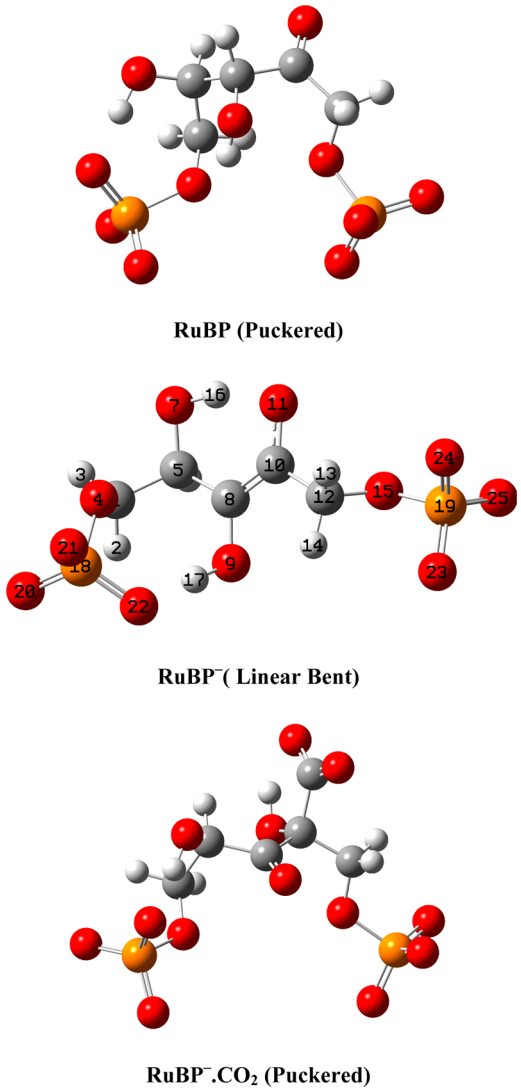

Figure 6. Optimized geometries of RuBP, $RuBP^-$, and $RuBP^-{\cdot}CO_2$, obtained from SCRF-PCM calculation using M06-2X functional and 6-311++G(3df,3pd) basis set.

aqueous medium, in the absence of Mg^{2+} cation. It has been calculated using a different functional with a different basis set.

We consider the equilibria (eq S1) along with the autoionization of water:

$$H_2O = H^+(aq) + OH^-(aq) \quad (K_w = 1.0 \times 10^{-14}) \qquad (25)$$

This gives $[H_2CO_3] = K_h[CO_2]$, $[HCO_3^-] = K_{a1}K_h[CO_2]/[H^+]$, and $[CO_3^{2-}] = K_{a2}[HCO_3^-]/[H^+]$. The charge balance is attained due to the presence of positive ions other than H^+, such as Mg^{2+}.[53] However, the concentration of other ions does not directly enter into the calculation. The values of equilibrium constants and eq S3 have been used to estimate $[CO_2]$ for Table 5. As such the ionization constant of water pinpoints the pH of the solution, and it too does not directly enter into the calculation.

The bundle sheath is known to have an average pH of 7.6. At this pH, the $CO_2(aq):H_2CO_3(aq):HCO_3^-(aq):CO_3^{2-}(aq)$ concentration ratios are 1:0.0017:16.92:0.0316, so the presence of CO_3^{2-} hardly alters the calculated results. Typical experimental data are available from ref 54. The total inorganic carbon (CO_2, H_2CO_3, HCO_3^-, and CO_3^{2-}) concentration

Table 5. Concentrations of Total Inorganic Carbon (TIC), Solvated Carbon Dioxide, Solvated $RuBP^-{\cdot}CO_2$ Complex, and the Effective CO_2 Concentration in Bundle Sheath of Different C_4 Plant Species

species	$[CO_2]_{TIC}$ mM[a]	$[CO_2]$ mM[b]	$[RuBP^-{\cdot}CO_2]$ mM[c]	$[CO_2]_{eff}$ mM[d]	$[CO_2]_{eff}/[CO_2]_{TIC}$
E. crusgalli	0.37	0.0206	5.9992	6.369	17.2
S. vulgare	0.16	0.0089	5.9982	6.158	38.5
E. indica	0.77	0.0430	5.9996	6.770	8.8
P. miliaceum	0.35	0.0195	5.9992	6.349	18.1
U. panioides	0.99	0.0552	5.9997	6.990	7.1
P. maximum	0.83	0.0463	5.9996	6.830	8.2

[a]Calculated from pool size taking that the bundle sheath cell volume is 19% of volume of leaf. See ref 35. [b]Estimated using pH = 7.6. [c]From eq 26, using $[RuBP]_{tot}$ = 6 mM, ref 55. [d]$[CO_2]_{eff} = [CO_2]_{TIC} + [RuBP^-.CO_2]$.

(TIC) in bundle sheath cells has been determined by Furbank and Hatch[35] for different C_4 plants. The concentration of total RuBP in the maize leaves was reported by Usuda[55] as 6 mM, about 2 times above the estimated RuBP binding-site concentration on ribulose bisphosphate carboxylase-oxygenase (Rubisco) of 2.6 mM in (maize) bundle sheath chloroplasts in the presence of light. From reactions 23 and 24, the concentration of the $RuBP^-{\cdot}CO_2$ complex is given by

$$[RuBP^-{\cdot}CO_2] = \frac{K_1K_2[OH^-][CO_2]}{1 + K_1[OH^-] + K_1K_2[OH^-][CO_2]}[RuBP]_{tot} \qquad (26)$$

The effective concentration $[CO_2]_{eff} = [CO_2]_{TIC} + [RuBP^-{\cdot}CO_2]$ is calculated in Table 5. The ratio $[CO_2]_{eff}:[CO_2]_{TIC}$ is observed to vary between 7.1 and 38.5. Thus, a substantially large amount of CO_2 is stored as the $RuBP^-{\cdot}CO_2$ complex and is readily available for the formation of 3-PGA, thereby enhancing the rate of photosynthesis.

CONCLUSIONS

Dissolution of carbon dioxide is a complex process. It is not energetically favorable, not even when thermal corrections are included. One has to consider the effect of hydrogen bonding accompanied by loss of phonon energy. Finally, one finds that the entropy of mixing in the aqueous phase plays the dominant role. When all these effects are taken into consideration, one can predict the solubility with reasonable accuracy. Increase in dielectric constant tends to increase the solubility: the internal energy has the greater say when hydrogen bonding and phonon contributions remain more or less unchanged.

Another interesting feature established in this work is that the effective rise in concentration of carbon dioxide inside bundle sheath cells of C_4 plants is due to an abundant supply from surrounding mesophylls and an efficient storage mechanism involving complexation with the dienolate form of $RuBP^-$. This enhances the rate of photosynthesis.

ASSOCIATED CONTENT

Supporting Information

Related analytical chemistry calculations; tables of optimized energies, C=O bond length, hydrogen bond energy, and vibrational frequencies; and full reference 36. This material is available free of charge via the Internet at http://pubs.acs.org.

dx.doi.org/10.1021/jp505237s | J. Phys. Chem. B 2014, 118, 8782−8791

AUTHOR INFORMATION

Corresponding Author

*E-mail: sndatta@chem.iitb.ac.in.

Notes

The authors declare no competing financial interest.

ACKNOWLEDGMENTS

The authors are grateful to the Council of Scientific and Industrial Research for financial support of this work. We acknowledge the IIT Bombay computer center for making their facilities available to us.

REFERENCES

(1) Dodds, W. S.; Stutzman, L. F.; Sollami, B. J. Carbon Dioxide Solubility in Water. *Ind. Eng. Chem.* **1956**, *1*, 92−95.

(2) Jönsson, B.; Karlström, G.; Wennerström, H. Ab Initio Molecular Orbital Calculations on the Water−Carbon Dioxide System: Molecular Complexes. *Chem. Phys. Lett.* **1975**, *30*, 58−59.

(3) Nguyen, M. T.; Raspoet, G.; Vanquickenborne, L. G. How Many Water Molecules are Actively Involved in the Neutral Hydration of Carbon Dioxide? *J. Phys. Chem. A* **1997**, *101*, 7379−7388.

(4) Nir, S.; Adams, S.; Rein, R. Polarizibility Calculations on Water, Hydrogen, Oxygen, and Carbon Dioxide. *J. Chem. Phys.* **1973**, *59*, 3341−3355.

(5) Baltrusaitis, J.; Schuttlefield, J. D.; Zeitler, E.; Jensen, J. H.; Grassian, V. H. Surface Reactions of Carbon Dioxide at the Adsorbed Water−Oxide Interface. *J. Phys. Chem. C* **2007**, *111*, 14870−14880.

(6) Rustad, J. R.; Nelmes, S. L.; Jackson, V. E.; Dixon, D. A. Quantum-Chemical Calculations of Carbon-Isotope Fractionation in CO_2(g), Aqueous Carbonate Species, and Carbonate Minerals. *J. Phys. Chem. A* **2008**, *112*, 542−555.

(7) Zeebe, R. E. Hydration in Solution is Critical for Stable Oxygen Isotope Fractionation between Carbonate Ion and Water. *Geochim. Cosmochim. Acta* **2009**, *73*, 5283−5291.

(8) Brodholt, J.; Wood, B. Molecular Dynamics Simulations of the Properties of CO_2−H_2O Mixtures at High Pressure and Temperature. *Am. Mineral.* **1993**, *78*, 558−564.

(9) Salaniwal, S.; Cui, S. T.; Cochran, H. D.; Cummings, P. T. Molecular Simulation of a Dichain Surfactant/Water/Carbon Dioxide System. 1. Structural Properties of Aggregates. *Langmuir* **2001**, *17*, 1773−1783.

(10) Kuznetsova, T.; Kvamme, B. Thermodynamic Properties and Interfacial Tension of a Model Water−Carbon Dioxide System. *Phys. Chem. Chem. Phys.* **2002**, *4*, 937−941.

(11) Saharay, M.; Balasubramanian, S. Ab Initio Molecular Dynamics Investigations of Structural, Electronic, and Dynamical Properties of Water in Supercritical Carbon Dioxide. *Ind. J. Phys.* **2009**, *83*, 13−29.

(12) Velaga, S.; Vedam, V.; Anderson, B. J. Molecular Dynamics Studies of the Stability of CO_2 and CH_4 Hydrates in the Presence of Unsaturated Fluids. *Proceedings of the 7th International Conference on Gas Hydrates (ICGH 2011)*, Edinburgh, Scotland, UK, July 17−21, 2011.

(13) Zeebe, R. E. On the Molecular Diffusion Coefficients of Dissolved CO_2, HCO_3^-, and CO_3^{2-} and Their Dependence on Isotopic Mass. *Geochim. Cosmochim. Acta* **2011**, *75*, 2483−2498.

(14) Perez-Blanco, M. E.; Maginn, E. J. Molecular Dynamics Simulations of Carbon Dioxide and Water at an Ionic Liquid Interface. *J. Phys. Chem. B* **2011**, *115*, 10488−10499.

(15) Harris, J. G.; Yung, K. H. Carbon Dioxide's Liquid−Vapor Coexistence Curve and Critical Properties As Predicted by a Simple Molecular Model. *J. Phys. Chem.* **1995**, *99*, 12021−12024.

(16) Vaida, V. Perspective: Water Cluster Mediated Atmospheric Chemistry. *J. Chem. Phys.* **2011**, *135*, 020901 (1−8).

(17) Van Der Meer, D. G.; Zeebe, R. E.; Hinsbergen, D. J. J.; Sluijs, A.; Spakman, W.; Torsvik, T. H. Plate Tectonic Controls on Atmospheric CO_2 Levels Since the Triassic. *Proc. Natl. Acad. Sci. U.S.A.* **2014**, *111* (12), 4380−4385.

(18) Gallet, G. A.; Pietrucci, F.; Andreoni, W. Bridging Static and Dynamical Descriptions of Chemical Reactions: An Ab Initio Study of CO_2 Interacting with Water Molecules. *J. Chem. Theory Comput.* **2012**, *8*, 4029−4039.

(19) Galib, M.; Hanna, G. Mechanistic Insights into the Dissociation and Decomposition of Carbonic Acid in Water via the Hydroxide Route: An Ab Initio Metadynamics Study. *J. Phys. Chem. B* **2011**, *115*, 15024−15035.

(20) Galib, M.; Hanna, G. The Role of Hydrogen Bonding in the Decomposition of H_2CO_3 in Water: Mechanistic Insights from Ab Initio Metadynamics Studies of Aqueous Clusters. *J. Phys. Chem. B* **2014**, *118*, 5983−5993.

(21) Stirling, A.; Pápai, I. H_2CO_3 Forms via HCO_3^- in Water. *J. Phys. Chem. B* **2010**, *114*, 16854−16859.

(22) Wang, B.; Cao, Z. How Water Molecules Modulate the Hydration of CO_2 in Water Solution: Insight from the Cluster-Continuum Model Calculations. *J. Comput. Chem.* **2013**, *34*, 372−378.

(23) Stirling, A. HCO_3^- Formation from CO_2 at High pH: Ab Initio Molecular Dynamics Study. *J. Phys. Chem. B* **2011**, *115*, 14683−14687.

(24) Panhuis, M. I. H.; Patterson, C. H.; Lynden-Bell, R. M. A Molecular Dynamics Study of Carbon Dioxide in Water: Diffusion, Structure and Thermodynamics. *Mol. Phys.* **1998**, *94*, 963−972.

(25) Leung, K.; Nielsen, I. M. B.; Kurtz, I. *Ab Initio* Molecular Dynamics Study of Carbon Dioxide and Bicarbonate Hydration and the Nucleophilic Attack of Hydroxide on CO_2. *J. Phys. Chem. B* **2007**, *111*, 4453−4459.

(26) López-Rendón, R.; Alejandre, J. Molecular Dynamics Simulations of the Solubility of H_2S and CO_2 in Water. *J. Mex. Chem. Soc.* **2008**, *52*, 88−92.

(27) Kumar, P. P.; Kalinichev, A. G.; Kirkpatrick, R. J. Hydrogen-Bonding Structure and Dynamics of Aqueous Carbonate Species from Car−Parrinello Molecular Dynamics Simulations. *J. Phys. Chem. B* **2009**, *113*, 794−802.

(28) Moin, S. T.; Pribil, A. B.; Lim, L. H. V.; Hofer, T. S.; Randolf, B. R.; Rode, B. M. Carbon Dioxide in Aqueous Environment—A Quantum Mechanical Charge Field Molecular Dynamics Study. *Int. J. Quantum Chem.* **2011**, *111*, 1370−1378.

(29) Galamba, N. On the Effects of Temperature, Pressure, and Dissolved Salts on the Hydrogen-Bond Network of Water. *J. Phys. Chem. B* **2013**, *117*, 589−601; Correction to On the Effects of Temperature, Pressure and Dissolved Salts on the Hydrogen-bond Network of Water. *J. Phys. Chem. B* **2013**, *117*, 5792−5792.

(30) Srivastava, A.; Alleman, C.; Ghosh, S.; Lee, L. J. Molecular Dynamics Simulation Based Evaluation of Glass Transition Temperatures of Polystyrene in the Presence of Carbon Dioxide. *Modell. Simul. Mater. Sci. Eng.* **2010**, *18*, 065003 (1−22).

(31) Alleman, C.; Srivastava, A.; Ghosh, S. Molecular Dynamics Simulations of the Effects of Carbon Dioxide on the Interfacial Bonding of Polystyrene Thin Films. *J. Polym. Sci. B: Polym. Phys.* **2011**, *49*, 1183−1194.

(32) Lawlor, D. H. *Photosynthesis: Metabolism, Control and Physiology*; ELBS-Longman: Singapore, 1989; pp 184−192.

(33) Portis, A. R.; Parry, M. A. J. Discoveries in Rubisco (Ribulose 1,5-bisphosphate carboxylase/oxygenase): A Historical Perspective. *Photosynth. Res.* **2007**, *94*, 121−143.

(34) Cleland, W. W.; Andrews, T. J.; Gutteridge, S.; Hartman, F. C.; Lorimer, G. H. Mechanism of Rubisco: The Carbamate as General Base. *Chem. Rev.* **1998**, *98*, 549−561.

(35) Furbank, R. T.; Hatch, M. D. Mechanism of C4 Photosynthesis: The Size and Composition of the Inorganic Carbon Pool in Bundle Sheath Cells. *Plant Physiol.* **1987**, *85*, 958−964.

(36) Frisch, M. J.; Trucks, G. W.; et al. *Gaussian 09*, revision A.02; Gaussian, Inc.: Wallingford, CT, 2009.

(37) Wagner, W.; Pruss, A. Addendum to International Equations for the Saturation Properties of Ordinary Water Substance. Revised According to the International Temperature Scale of 1990. *J. Phys. Chem. Ref. Data* **1987**, *16*, 893; *J. Phys. Chem. Ref. Data* **1993**, *22*, 783−787.

(38) Zhao, Y.; Truhlar, D. G. The M06 Suite of Density Functionals for Main Group Thermochemistry, Thermochemical Kinetics, Noncovalent Interactions, Excited States, and Transition Elements: Two New Functionals and Systematic Testing of Four M06-Class Functionals and 12 Other Functionals. *Theor. Chem. Acc.* **2008**, *120*, 215−241.
(39) Zhao, Y.; Truhlar, D. G. Density Functionals with Broad Applicability in Chemistry. *Acc. Chem. Res.* **2008**, *41*, 157−167.
(40) Liu, Y.; Zhao, J.; Li, F.; Chen, Z. Appropriate Description of Intermolecular Interactions in the Methane Hydrates. *J. Comput. Chem.* **2013**, *34*, 121−131.
(41) Mourik, T.; Gdanitz, R. J. A. Critical Note on Density Functional Theory Studies on Rare-Gas Dimers. *J. Chem. Phys.* **2002**, *116*, 9620−9623.
(42) Walker, M.; Harvey, A. J. A.; Sen, A.; Dessent, C. E. H. Performance of M06, M06-2X, and M06-HF Density Functionals for Conformationally Flexible Anionic Clusters: M06 Functionals Perform Better than B3LYP for a Model System with Dispersion and Ionic Hydrogen-Bonding Interactions. *J. Phys. Chem. A* **2013**, *117*, 12590−12600.
(43) Mardirossian, N.; Lambrecht, D. S.; McCaslin, L.; Xantheas, S. S.; Head-Gordon, M. The Performance of Density Functionals for Sulfate−Water Clusters. *J. Chem. Theory Comput.* **2013**, *9*, 1368−1380.
(44) Jones, G. J.; Robertazzi, A.; Platts, J. A. Efficient and Accurate Theoretical Methods to Investigate Anion−Pi Interactions in Protein Model Structures. *J. Phys. Chem. B* **2013**, *117*, 3315−3322.
(45) Morgado, C. A.; Jurecka, P.; Svozil, D.; Hobza, P.; Sponer, J. Reference MP2/CBS and CCSD(T) Quantum-Chemical Calculations on Stacked Adenine Dimers. Comparison With DFT-D, MP2.5, SCS (MI)-MP2, M06-2X, CBS(SCS-D) and Force Field Descriptions. *Phys. Chem. Chem. Phys.* **2010**, *12*, 3522−3534.
(46) Smith, S. A.; Hand, K. E.; Love, M. L.; Hill, G.; Magers, D. H. Conventional Strain Energies of Azetidine and Phosphetane. *J. Comput. Chem.* **2013**, *34*, 558−565.
(47) Simon, A.; Peters, K. Single−Crystal Refinement of the Structure of Carbon Dioxide. *Acta Cryst. B* **1980**, *36*, 2750−2751.
(48) Ding, Y.; Macko, P.; Romanini, D.; Perevalov, V. I.; Tashkun, S. A.; Teffo, J. L.; Hu, S. M.; Campargue, A. High Sensitivity cw-Cavity Ringdown and Fourier Transform Absorption Spectroscopies of $^{13}CO_2$. *J. Mol. Spectrosc.* **2004**, *226*, 146−160.
(49) Housecroft, C.; Sharpe, A. G.; *Inorganic Chemistry*, 2nd ed.; Prentice-Pearson-Hall: Upper Saddle River, NJ, 2005; p 368.
(50) Greenwood, N. N.; Earnshaw, A. *Chemistry of the Elements*, 2nd ed.; Butterworth-Heinemann: Oxford, U.K., 1997; pp 310.
(51) Wang, X.; Conway, W.; Burns, R.; McCann, N.; Maeder, M. Comprehensive Study of the Hydration and Dehydration Reactions of Carbon Dioxide in Aqueous Solution. *J. Phys. Chem. A* **2010**, *114*, 1734−1740.
(52) El-Hendawy, M. M.; Garate, J. A.; English, N. J.; O'Reilly, S.; Mooney, D. A. Diffusion and Interactions of Carbon Dioxide and Oxygen in the Vicinity of the Active Site of Rubisco: Molecular Dynamics and Quantum Chemical Studies. *J. Chem. Phys.* **2012**, *137*, 145103 (1−10).
(53) Edwards, G.; Walker, D. A. *C3, C4-Mechanisms, and Cellular and Enviromental Regulation, of Photosynthesis*, 1st ed.; Blackwell Scientific Publications: Oxford, U.K., 1983; pp 112−114.
(54) Furbank, R. T.; Jenkins, C. L. D.; Hatch, M. D. CO_2 Concentrating Mechanism of C_4 Photosynthesis Permeability of Isolated Bundle Sheath Cells to Inorganic Carbon. *Plant Physiol.* **1989**, *91*, 1364−1371.
(55) Usuda, H. Changes in Levels of Intermediates of the C4 Cycle and Reductive Pentose Phosphate Pathway under Various Light Intensities in Maize Leaves. *Plant Physiol.* **1987**, *84*, 549−554.